

Surface Crystallization of Liquid Normal-Alkanes

X. Z. Wu,⁽¹⁾ E. B. Sirota,⁽¹⁾ S. K. Sinha,⁽¹⁾ B. M. Ocko,⁽³⁾ and M. Deutsch^{(2),(3)}

⁽¹⁾*Corporate Research Science Laboratory, Exxon Research and Engineering Company, Route 22 East, Annandale, New Jersey 08801*

⁽²⁾*Physics Department, Bar Ilan University, Ramat Gan 52900, Israel*

⁽³⁾*Physics Department, Brookhaven National Laboratory, Upton, New York 11973*

(Received 17 November 1992)

X-ray scattering and surface tension measurements reveal the formation of a crystalline monolayer on the surface of liquid n -alkanes at about 3 °C above the bulk solidification temperature. The molecules in the monolayer are hexagonally packed and oriented normal to the surface. The single solid monolayer persists down to the bulk solidification temperature, thus exhibiting a very limited partial wetting.

PACS numbers: 68.10.-m, 61.25.Eg, 64.70.Dv

Linear hydrocarbon chains, known as n -alkanes [CH_3 - $(\text{CH}_2)_{n-2}$ - CH_3 , denoted C n], are among the most basic building blocks of organic matter. They form part of organic and biological molecules like lipids, surfactants, and liquid crystals, and determine their properties to a large extent. As major constituents of oils, fuels, polymers, and lubricants they also have an immense industrial importance. Their bulk structure and properties have been extensively studied [1,2], revealing a rich phase behavior. The properties of alkanes at surfaces are currently of great interest [3-5]. However, their free surface structures have not been hitherto measured on an Å scale. Studies of molecules incorporating alkanelike tails, in particular liquid crystals [6-8], surfactants on water [9], and alkane thiols on gold [10] reveal a variety of unique effects including distinct surface phases, partial wetting, and quasi-2D crystal formation at the surface. Our x-ray scattering and surface tension measurements, reported here, show conclusively the abrupt formation of a crystalline monolayer on the surface of n -alkanes above their bulk melting temperatures. This appears to be the simplest system in which surface-induced 2D crystalline ordering has been observed. The surface ordering found here is fundamentally different from that of Langmuir films on water where the insolubility of the amphiphile molecules confines them to the surface facilitating in-plane ordering. In this system there is a free exchange of molecules between the surface and the bulk. Our surface tension results, analyzed in terms of a simple thermodynamical model, lend further support to the x-ray findings.

X-ray reflectivity (XR) and grazing incidence diffraction (GID) measurements were carried out on the free surface of C18, C20, and C24, whose bulk solidification temperatures T_m are given in Table I. The sample [11] consisted of a ~ 0.5 mm thick alkane film on a 3 in. silicon wafer. This was placed inside a sealed cell whose temperature was regulated and uniform to within a few mK. The measurements were carried out on the Harvard-BNL Liquid Surface Diffractometer at the National Synchrotron Light Source, Brookhaven National

Laboratory, beam line X22B with a wavelength of $\lambda = 1.547$ Å.

For x rays incident at a grazing angle α on a liquid surface the reflectivity is given by [12,13]

$$R(q_z)/R_F(q_z) = \left| \frac{1}{\rho_\infty} \int_{-\infty}^{\infty} [\partial \rho(z)/\partial z] \exp(iq_z z) dz \right|^2, \quad (1)$$

where $\rho(z)$ is the electron density profile averaged over the horizontal coherence area of the beam, ρ_∞ is the electron density deep in the bulk, $q_z = (4\pi/\lambda) \sin \alpha$ is the vertical momentum transfer, and R_F is the Fresnel reflectivity of an ideally flat and abrupt surface. Thus, reflectivity provides information on the structure normal to the surface. Below the critical angle for total external reflection, $\alpha_c = \lambda(\rho_\infty r_0/\pi)^{1/2}$ ($r_0 = 2.82 \times 10^{-5}$ Å), the refracted beam is evanescent, penetrating only to a few molecular lengths and traveling along the surface. Scattering of this wave (GID) provides information on the in-plane structure of the interface and is virtually free from the much stronger scattering of the bulk which occurs for $\alpha > \alpha_c$.

The reflectivities obtained at temperatures $T \approx T_m$

TABLE I. Measured properties and fit parameters for n -alkanes. Values marked by * were kept fixed in the fit, and those marked † were constrained to be the same. For notation see text.

	C18	C20	C24
	Measured		
T_m (°C)	27.3	35.6	50.0
T_s (°C)	30.0	38.6	53.1
ΔT (°C)	2.7	3.0	3.1
	Liquid phase fit		
σ (Å)	4.7	4.1	4.3
	Monolayer phase fit: One-slab model		
ρ_L ($e/\text{Å}^3$)	0.268*	0.268*	0.268*
ρ ($e/\text{Å}^3$)	0.321†	0.321†	0.321†
D (Å)	19.6	21.9	26.5
σ_1 (Å)	3.8	3.9	4.3
σ_2 (Å)	1.0*	1.0*	1.0*

+4°C are plotted as circles in Fig. 1. No variation is observed in the shape of the curves up to $T_m + 20^\circ\text{C}$, and the observed a_c is consistent with the bulk $\rho_L = 0.268 \text{ e}/\text{\AA}^3$ [1]. The reflectivity curves have a shape characteristic of simple liquids where $R(q_z)/R_F(q_z) = \exp(-\sigma^2 q_z^2)$ and σ is the "effective" interfacial width [13]. Fits of this form to our data are shown by the solid lines in Fig. 1, indicating excellent agreement. The fit parameters are listed in Table I. For simple liquids, σ was shown [13] to be dominated by the thermally induced capillary wave amplitudes, which are proportional to $\gamma^{-1/2}$, where γ is the surface tension. From previous measurements on H_2O [14] with a similar geometry where $\gamma_{\text{H}_2\text{O}} = 72 \text{ dyn/cm}$, $\sigma_{\text{H}_2\text{O}} \approx 2.7 \text{ \AA}$, and our measured $\gamma_{\text{C}_{20}} \approx 28 \text{ dyn/cm}$ (see below), we calculate for alkanes $\sigma_{\text{C}_n} = \sigma_{\text{H}_2\text{O}}(\gamma_{\text{H}_2\text{O}}/\gamma_{\text{C}_n})^{1/2} \approx 4.3 \text{ \AA}$, in very good agreement with the fitted values in Table I.

Below a critical surface temperature $T_s \approx T_c + 3^\circ \text{C}$ (listed in Table I) a higher density layer is formed at the surface, as indicated by the modulated reflectivity curves shown by squares in Fig. 1. The curves are found to be temperature independent for $T_m < T < T_s$. The modulated reflectivities result from interference of the waves reflected from the top and bottom of the surface layer.

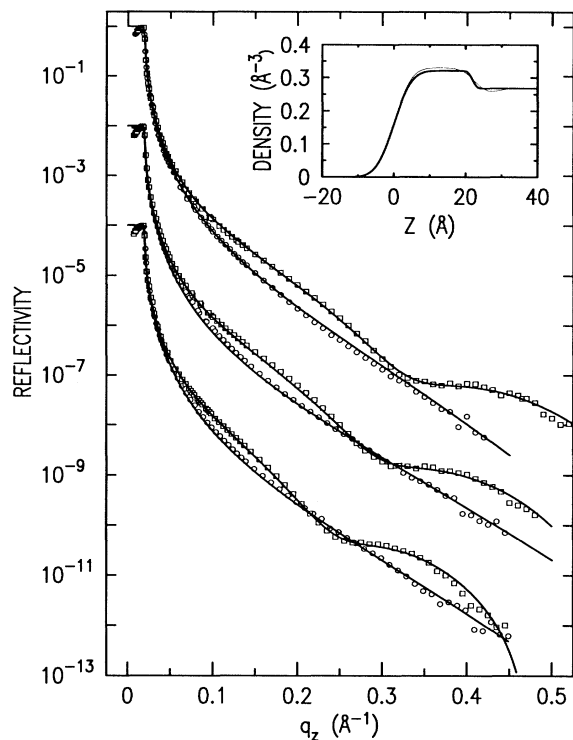


FIG. 1. Reflectivities for C18, C20, and C24. The data for the liquid surface phase are shown by open circles and those for the surface monolayer phase by open squares. The curves are shifted by two decades each for better visibility. Inset: The model surface electron density profiles for the one-slab (thick) and two-slab (thin) models. The depletion layer is clearly seen.

The simplest model for the density profile of this layer is a slab of thickness D and density $\rho \neq \rho_L$. The modulation period is $\Delta q = 2\pi/D$ and the amplitude is determined by $\rho - \rho_L$. Two interfacial widths σ_1 and σ_2 , representing the vapor and liquid interfaces, respectively, are also included in the model. The calculated reflectivities, shown as solid lines in Fig. 1, provide good agreement with the data for the monolayer phase. The fitted density profile for C20 is shown as the solid line in the inset of Fig. 1 and the corresponding parameters are listed in Table I. The surface layer density, $0.321 \text{ e}/\text{\AA}^3$, is found to be 20% higher than that of the bulk liquid alkane and is comparable to the $[-\text{CH}_2]_{n-2}$ part density of the rotator phases [1], which occur in bulk Cn between the low-temperature crystal phase and the liquid phase. The fitted D values, listed in Table I, are shorter by $\sim 2 \text{ \AA}$ than the corresponding first-to-last carbon distances, calculated using the literature value of 1.27 \AA per bond [1]. To a large extent, this discrepancy is due to the simplicity of the model. The possibility of contributions from nonrigidity, local tilt, and gauche kinks in the chain cannot be ruled out.

A more realistic model has to take into account the reduced density of the CH_3 group. This is modeled by adding a lower density slab at the liquid interface. The analogous effect at the vapor interface is absorbed into the surface roughness parameter σ_1 . The depletion layer effectively rotates the phase of the wave reflected from the monolayer-liquid interface increasing the fitted value of the surface layer thickness D . Further details will be published elsewhere [15]. The limited q_z range of the measurements imposed by the signal-to-noise ratio does not permit a clear choice of one model over the other. The data do show, however, that the surface layer has a density close to that of the bulk rotator phases, its upper and lower boundaries are sharply defined, and its thickness closely corresponds to that of a straight chain point-

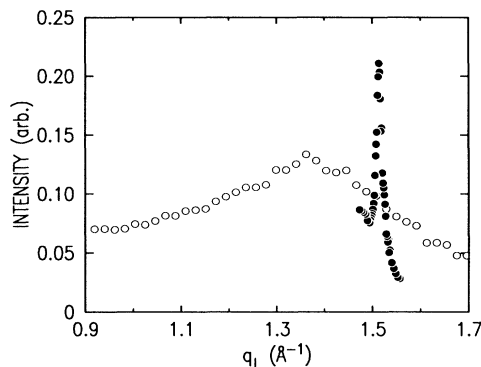


FIG. 2. The in-plane diffraction of the C20 alkane liquid. At high temperature, only the liquid bulk peak (open circles) is observed. The formation of the surface crystalline monolayer is manifested by a drop in the intensity of the liquid peak and the appearance of a resolution-limited Bragg peak (solid circle).

ed normal to the surface.

GID measurements were carried out to determine the in-plane order of the monolayer. The measurements for C20 are shown in Fig. 2 at temperatures above (open circles) and below (solid circles) T_s . The broad peak at $q_{\parallel}=1.35 \text{ \AA}^{-1}$ has a width of 0.35 \AA^{-1} (FWHM) and is typical of liquid alkanes. This yields a nearest-neighbor chain distance of $4\pi/1.35\sqrt{3}=5.37 \text{ \AA}$ and a short-range correlation length of about 3 molecular diameters. When the monolayer phase appears at T_s , the intensity of the liquid peak drops and a sharp peak appears at $q_{\parallel}=1.513 \text{ \AA}^{-1}$. Within our resolution, the peak position did not change with temperature. This "Bragg peak" clearly originates from the long-range positional order of the more densely packed surface layer [16]. It is resolution limited, implying a domain size larger than 1000 \AA . However, the measured mosaic distribution [17] indicates that it may be as large as a few millimeters. While the presence of other diffraction peaks cannot entirely be ruled out, no others were found for $q_{\parallel}<2.5 \text{ \AA}^{-1}$ and $q_z<1.4 \text{ \AA}^{-1}$. The peak position is consistent with that of the rotator R_{\parallel} phase [1], where the molecules are oriented on average normal to the layer and packed hexagonally. Assuming hexagonal packing for our monolayer, the area per chain is $(8\pi^2/\sqrt{3})/1.513^2=19.9 \text{ \AA}^2$, and the density of the central portion of the chain, $8/(1.27\times 19.9)=0.317 \text{ e/\AA}^3$, compares favorably with the value of 0.321 e/\AA^3 determined from the reflectivity fits.

To further characterize the monolayer, the temperature dependence of the reflectivity was measured at a fixed q_z for all three alkanes. A slow temperature scan ($0.05^\circ\text{C}/\text{min}$), at a $q_z=0.20 \text{ \AA}^{-1}$, is shown in Fig. 3(a). The abrupt formation of the dense surface layer is clearly seen at $T_s=38.6^\circ\text{C}$. Careful measurements, ensuring equilibrium conditions, indicate that this transition is of first order with little hysteresis in temperature. The bulk liquid-solid transition is manifested at $T_m=35.6^\circ\text{C}$ by the vanishing reflectivity due to the macroscopic surface roughening. $\Delta T=T_s-T_m$ is similar for the three samples and is given in Table I. The formation of a crystalline surface layer in n -alkanes is similar to the surface-induced order observed in liquid crystals [6-8]. It is important to note that below and above the surface transition, our reflectivity is seen to be independent of the temperature, and no continuous or discrete growth of the thickness of the surface layer is observed. This is in contrast with the liquid crystal 12CB, where growth of up to 5 surface smectic layers was observed upon approaching the bulk isotropic-smectic transition temperature [6], and the liquid crystal 9O.4 which shows complete wetting of the smectic- A phase by a 2D hexatic phase [8]. The solid alkane layer exhibits, therefore, a very limited partial wetting of the bulk liquid upon approaching the solidification temperature.

We have also carried out surface tension measurements

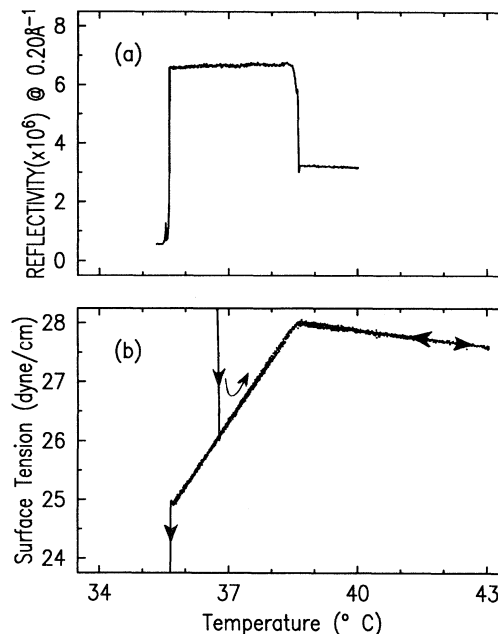


FIG. 3. (a) Temperature scan of the reflectivity of C20 at a fixed $q_z=0.20 \text{ \AA}^{-1}$. Note the abrupt changes on solidification, $T_m=35.6^\circ\text{C}$, and surface layer formation, $T_s=38.6^\circ\text{C}$. (b) Surface tension of C20 in heating and cooling cycles. The arrows denote the temperature scan direction. Note the hysteresis in the bulk melting and solidification, and its absence in the surface layer formation temperature.

employing the Wilhelmy plate method [18] using a thin roughened platinum plate 2.5 cm wide which is completely wet by the alkanes in the x-ray cell. The cell was modified for these measurements by making a small hole in the top to pass the wire carrying the Wilhelmy plate. As the vapor pressure of alkanes near melting is very low, the presence of the hole had a negligible influence on our results, as indicated by the close agreement of our data with previous measurements above T_s . The surface tension of C20 versus temperature is shown in Fig. 3(b) for both cooling and heating cycles. An abrupt change of slope at 38.6°C indicates the solid monolayer formation. Similar slope changes, arising from ordering at the surface, were observed in SDS/water solutions [19] and liquid metals [20]. Below the bulk alkane solidification temperature 35.6°C , a meaningful surface tension measurement is no longer possible. For all three samples, the phase transition temperatures obtained from the surface tension measurements are in agreement with those obtained from the x-ray reflectivity. Similar behavior was found in our surface tension study of alkanes from C16 to C44 [15]. Surprisingly, the effects reported here were not detected in any of the many earlier surface tension measurements [1,21] in alkanes. The only exceptions are the very recent surface tension measurements of Earnshaw and Hughes [5] on C15 to C18, which show a surface

phase transition. However, the nature of the surface phase was not elucidated in that study.

The abrupt change in the slope of the surface tension at T_s is easy to understand in terms of the relevant entropies. The surface tension slope is related to the bulk, S_b , and surface, S_s , entropies by $d\gamma/dT \sim -(S_s - S_b)$ [20]. For a liquid surface $S_s > S_b$, the difference being small. Thus, $d\gamma/dT \approx \text{const} < 0$ for simple liquids and alkanes above T_s as seen in Fig. 3(b). For C24, for example, we measured $-0.088 \text{ dyn/cm}^\circ\text{C}$ [15]. Upon formation of the crystalline monolayer, S_s is reduced below S_b , so that $d\gamma/dT > 0$, as is indeed observed below T_s in Fig. 3(b). Approximating S_s by the entropy of the bulk rotator phase, S_r , and using $S_r - S_b = 1.68 \times 10^9 \text{ ergs/mol}^\circ\text{C}$ determined for C24 from latent heat measurements [1], one calculates a positive slope of $1.41 \text{ dyn/cm}^\circ\text{C}$ in excellent agreement with the measured slope [15] of $1.32 \text{ dyn/cm}^\circ\text{C}$. Assuming that $S_s - S_b$ in the rotator phase is comparable to that in the liquid phase, the calculated slope would be $1.41 - 0.088 = 1.32 \text{ dyn/cm}^\circ\text{C}$, an even closer agreement.

In summary, we have experimentally discovered a layering transition on the free surface of liquid alkanes at temperatures above their bulk solidification. The single monolayer formed in an apparently first-order transition, with very little hysteresis, is found to have crystalline order with hexagonally packed, vertically standing chains. Surface tension measurements interpreted using basic thermodynamical principles corroborate the x-ray findings. Further measurements to elucidate chain length effects and admixture behavior are in progress.

We wish to acknowledge helpful discussions with and help of M. W. Kim, B. H. Cao, and H. E. King. M.D. thanks the Department of Physics, Brookhaven National Laboratory, for its hospitality and a summer fellowship during which this research was initiated, and the U.S.-Israel Binational Foundation for support. Brookhaven National Laboratory is supported by the Division of Materials Research, U.S. Department of Energy, under Contract No. DE-AC02-76CH00016.

- [1] An excellent summary of the properties of n -alkanes can be found in D. M. Small, *The Physical Chemistry of Lipids* (Plenum, New York, 1986).
- [2] E. B. Sirota, H. E. King, Jr., G. J. Hughes, and W. K. Wan, *Phys. Rev. Lett.* **68**, 492 (1992); E. B. Sirota, H. E. King, Jr., D. M. Singer, and H. Shao, in *Complex Fluids*, edited by E. B. Sirota, D. Weitz, T. Witten, and J. Israelachvili, MRS Symposia Proceedings No. 248 (Materials Research Society, Pittsburgh, 1992); *J. Chem. Phys.* **98** (1993).
- [3] T. K. Xia, J. Ouyang, M. W. Ribarsky, and U. Landman, *Phys. Rev. Lett.* **69**, 1967 (1992).
- [4] L. Askadskaya and J. P. Rabe, *Phys. Rev. Lett.* **69**, 1395 (1992).

- [5] J. C. Earnshaw and C. J. Hughes, *Phys. Rev. A* **46**, R4494 (1992).
- [6] B. M. Ocko, *Phys. Rev. Lett.* **64**, 2160 (1990); B. M. Ocko, A. Braslau, P. S. Pershan, J. Als-Nielsen, and M. Deutsch, *Phys. Rev. Lett.* **57**, 94 (1986).
- [7] E. B. Sirota, P. S. Pershan, S. Amador, and L. B. Sorensen, *Phys. Rev. A* **35**, 2283 (1987); E. B. Sirota, P. S. Pershan, L. B. Sorensen, and J. Collet, *Phys. Rev. A* **36**, 2890 (1987).
- [8] B. D. Swanson, H. Strager, D. J. Tweets, and L. B. Sorensen, *Phys. Rev. Lett.* **62**, 909 (1989).
- [9] S. Grayer Wolf, L. Leiserowitz, M. Lahav, M. Deutsch, K. Kjaer, and J. Als-Nielsen, *Nature (London)* **328**, 63 (1987); K. Kjaer, J. Als-Nielsen, C. A. Helm, L. A. Laxhuber, and H. Möhwald, *Phys. Rev. Lett.* **58**, 2224 (1987); P. Dutta, J. B. Peng, B. Lin, J. B. Ketterson, M. Prakash, P. Georgopoulos, and S. Ehrlich, *Phys. Rev. Lett.* **58**, 2228 (1987).
- [10] P. Fenter, P. Eisenberger, and K. S. Liang (to be published).
- [11] C18 was obtained from Aldrich; C20 and C24 from Sigma. All were labeled 99% pure and were used as obtained. Our results were completely reproducible for samples from different sources, and upon cycling repeatedly through the melting point. As discussed in Ref. [5], these are strong indications against ascribing the layer to surface-active contaminants. The x-ray measurements, which show a sharply defined layer of uniform thickness closely correlated with n , virtually exclude the possibility of impurities which differ greatly in length from n .
- [12] P. S. Pershan, *Faraday Discuss. Chem. Soc.* **89**, 231 (1990). This form is valid within the first Born approximation. However, for the present system an exact calculation using the full dynamical theory yields indistinguishable results.
- [13] A. Braslau, P. S. Pershan, G. Swislow, B. M. Ocko, and J. Als-Nielsen, *Phys. Rev. A* **38**, 2457 (1988); M. K. Sanyal, S. K. Sinha, K. G. Huang, and B. M. Ocko, *Phys. Rev. Lett.* **66**, 628 (1991).
- [14] D. K. Schwartz, M. L. Schlossman, E. K. Kawamoto, G. J. Kellogg, P. S. Pershan, and B. M. Ocko, *Phys. Rev. A* **41**, 5687 (1990).
- [15] X. Z. Wu, E. B. Sirota, S. K. Sinha, B. M. Ocko, and M. Deutsch (to be published).
- [16] The data are not good enough to distinguish between quasi- and true long-range order.
- [17] M. L. Schlossman, D. K. Schwartz, P. S. Pershan, E. H. Kawamoto, G. J. Kellogg, and S. Lee, *Phys. Rev. Lett.* **66**, 1599 (1991).
- [18] G. L. Gaines, *Insoluble Monolayers at the Liquid Gas Interface* (Wiley, New York, 1966).
- [19] B. Berge, L. Fancheux, K. Schwab, and A. Libchaber, *Nature (London)* **350**, 322 (1991).
- [20] C. A. Croxton, *Statistical Mechanics of the Liquid Surface* (Wiley, New York, 1980).
- [21] F. D. Rossini, K. S. Pitzer, R. L. Arnett, R. M. Braun, and G. C. Pimentel, *Selected Values of Physical and Thermodynamic Properties of Hydrocarbons and Related Compounds* (Carnegie, Pittsburgh, 1953); J. Timmermans, *Physico-Chemical Constants of Pure Organic Compounds* (Elsevier, New York, 1965).